ACS OMEGA

Open Access

http://pubs.acs.org/journal/acsodf

Article

Magnetic Nanoparticles Stabilized by Phosphorylcholine-Containing Polymer for Label-Free C-Reactive Protein Detection

Tinnakorn Phuangkaew, Suttawan Saipai, Voravee P. Hoven, and Piyaporn Na Nongkhai*

Cite This: *ACS Omega* 2025, 10, 10317−10326

Read Online

ACCESS | Metrics & More | Article Recommendations | Supporting Information

ABSTRACT: This research aims to develop a simple yet effective assay for detecting C-reactive protein (CRP), based on magnetic nanoparticles functionalized with a phosphorylcholine-containing polymer. Magnetic nanoparticles stabilized with poly[(methacrylic acid)-*ran*-(methacryloyloxyethyl phosphorylcholine)] (PMAMPC-MNPs), were prepared by coprecipitation of ferric and ferrous salts in the presence of PMAMPC. Carboxyl groups in the methacrylic acid (MA) repeat units chelate with Fe atoms during MNPs formation, while the methacryloyloxyethyl phosphorylcholine (MPC) repeat units provide specifically binding sites and conjugate with CRP in the presence of Ca^{2+}, leading to the aggregation of PMAMPC-MNPs. The PMAMPC-MNPs were characterized by attenuated total reflectance-Fourier transform infrared spectroscopy (ATR-FTIR), transmission electron microscopy (TEM), dynamic light scattering (DLS), thermogravimetric analysis (TGA), and X-ray diffraction (XRD). To determine CRP detection with the naked eye, the precipitation of PMAMPC-MNPs in the presence of CRP and Ca^{2+} was monitored without an external magnetic field. Additionally, by taking advantage of the peroxidase-like activity of MNPs, the addition of 3,3′,5,5′-tetramethylbenzidine (TMB) and H_2O_2 to the supernatant of unbound PMAMPC-MNPs after magnetic separation allows for the colorimetric determination of CRP. This measurement is inversely proportional to the amount of CRP and is detected in an antibody-free system, with a linear range of 1−5 μg/mL and an experimental limit of detection (LOD) of 1.0 μg/mL. Moreover, 3 μg/mL CRP can also be detected in 50% diluted rabbit serum, covering the CRP cutoff level associated with the risk threshold for cardiovascular disease.

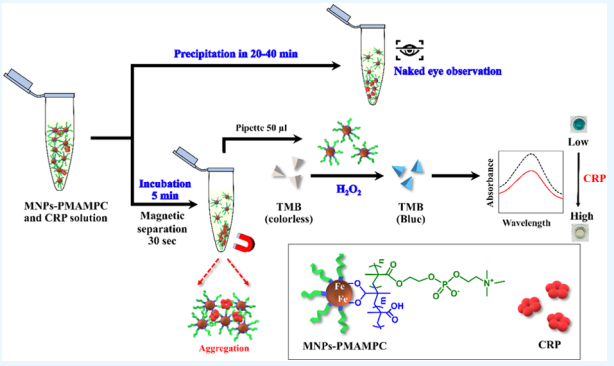

1. INTRODUCTION

The United Nations has set a goal to decrease the number of premature deaths caused by noncommunicable diseases, such as cardiovascular diseases including coronary heart disease and stroke, by one-third by 2030,[1] especially in elderly people, who are at greater risk of developing the disease than other age groups. The risk of cardiovascular diseases can be assessed by measuring the number of biomarkers in the blood such as homocysteine, cholesterol, and C-reactive protein (CRP).[2] The native CRP (nCRP) is a pentameric protein of which each subunit has a phosphocholine (PC) binding site and two calcium ions (Ca^{2+}). A blood CRP test, recommended by the American Heart Association, indicates high cardiovascular risk if CRP levels exceed 3.0 mg/L.[3,4] Currently, CRP assays can be performed in a laboratory using a variety of methods, including nephelometry,[5,6] immunoturbidimetry,[7,8] enzyme-linked immunosorbent assay (ELISA),[9−11] etc. These methods are highly effective, but they have limitations regarding analysis time, cost, inability to perform out-of-laboratory experiments, and the requirement for expertise in analysis.

2-Methacryloyloxyethyl phosphorylcholine (MPC)-based polymers have been widely employed in gene/drug delivery systems due to their excellent biocompatibility and are recognized as artificial cell membranes.[12−14] MPC with a cell-membrane mimic structure is utilized as a polymerizable specific ligand for CRP in the presence of calcium ions.[15] Poly(2-methacryloyloxyethyl phosphorylcholine) (PMPC) is one of the well-known zwitterionic polymers that can effectively suppress the nonspecific adsorption of other proteins in the presence of CRP. PMPC should thus be a potential and efficient artificial probe for selective antibody-free CRP sensors.[16−18] However, the current PMPC-based CRP sensor relies on specialized instruments for detection, including matrix-assisted laser desorption/ionization time-of-flight mass spectrometry (MALDI-TOF MS),[16] localized surface plasmon resonance (LSPR),[17] and electrochemical detection.[19] As a result, the development of instrument-free detection methods

Received: November 4, 2024
Revised: January 5, 2025
Accepted: March 3, 2025
Published: March 6, 2025

remains essential for creating novel diagnostic tools that can be rapidly and conveniently deployed.

Focusing on the properties of PMPC coating on particle surfaces such as gold nanoparticles (AuNPs) and magnetic nanoparticles (MNPs), aggregation of particles occurs after binding with CRP in the presence of Ca^{2+}, due to interparticle cross-linking. This aggregation phenomenon is detectable both by instrumental methods and by the naked eye. The thiol-terminated block copolymer of poly(2-methacryloyloxyethyl phosphorylcholine)-*b*-poly(*N*-methacryloyl-(L)-tyrosine methylester) (PMPC-*b*-PMAT) was synthesized and used for the synthesis and modification of AuNPs. These AuNPs exhibited good colloidal stability due to steric stabilization of the hydration layer of the copolymer. The C-reactive protein (CRP) detection was demonstrated using the aggregation of AuNPs through the binding of MPC to CRP in the presence of Ca^{2+}.[20] MNPs are inexpensive and widely recognized for their potential in biomagnetic separation. Fe_3O_4 nanoparticles exhibit great potential, especially for the rapid magnetic separation of protein, bacteria, and biomolecules, due to their response to magnetic field and large surface-to-volume ratio, which can induce efficient interactions with target analytes even in dilute samples containing various background materials.[21,22] Poly(MPC)-stabilized Fe_3O_4 nanoparticles (PMPC-MNPs) were prepared via hydrothermal method and surface-initiated atom transfer radical polymerization (SI-ATRP) of MPC.[21] Aggregation of PMPC-MNPs was induced after incubation with CRP in the presence of Ca^{2+}. The size change of PMPC-MNPs before and after CRP-induced aggregation can be monitored by dynamic light scattering (DLS). The simple synthesis of PMPC on MNPs was introduced by using poly[(methacrylic acid)-*ran*-(methacryloyloxyethyl phosphorylcholine)] (PMAMPC).[22,23] The PMAMPC, which contains methacrylic acid (MA) repeat units with carboxyl groups, allows the copolymer to easily chelate with Fe atoms during MNP formation, while the MPC repeat units provide biocompatibility and antifouling characteristics.[24−26]

There are many reports that use Fe_3O_4 nanocomposites to provide peroxidase-like activity in catalytic oxidation of 3,3,5,5′-tetramethylbenzidine (TMB) in the presence of H_2O_2, developing a color reaction suitable for instrument-free colorimetric detection.[23,27,28] The signal amplification is based on the catalytic ability of Fe_3O_4 nanoparticles to induce the oxidation of the organic substrate, resulting in a distinct color change (from colorless to blue) that can be easily monitored by either an instrument or even with the naked eye. The enzymatic-like activities of Fe_3O_4 nanoparticles enabled colorimetric detection of bacteria in food, including both Gram-negative *Escherichia coli* and Gram-positive *Staphylococcus aureus*.[29,30] Furthermore, the peroxidase-like activity of these magnetic nanoparticles has been studied for detecting metal ions[31] and glucose.[32]

Inspired by the aforementioned research, the goal of this research is to develop a sample, rapid, and effective method for CRP measurement based on magnetic separation of magnetic nanoparticles stabilized with phosphorylcholine (PC)-containing polymer, poly[(methacrylic acid)-*ran*-(methacryloyloxyethyl phosphorylcholine)] (PMAMPC-MNPs), which were prepared by coprecipitation of ferric and ferrous salts in the presence of PMAMPC. When calcium ions (Ca^{2+}) are present, the PMAMPC-MNPs in the tested solution would aggregate with CRP, leading to flocculation that can be visually observed in correlation with the CRP concentration. The CRP-PMAMPC-MNPs complex can then be concentrated using an external magnetic field. Additionally, CRP-free PMAMPC-MNPs are identified through a label-free colorimetric assay. Taking advantage of the peroxidase-like activity of MNPs, the signal was further amplified by introducing TMB as a substrate together with H_2O_2 in CRP-unbound PMAMPC-MNPs solution, which is measured by UV−vis spectroscopy. The detection of CRP in human serum samples was also demonstrated.

2. EXPERIMENTAL SECTION

2.1. Materials. Methacryloyloxyethyl phosphorylcholine (MPC) was purchased from NOF Corp. (Japan). Methacrylic acid (MA) supplied by TCI (Japan) was distilled under reduced pressure with added *p*-methoxyphenol (59 °C/13.5 mmHg). Ferrous chloride tetrahydrate ($FeCl_2{\cdot}4H_2O$), ferric chloride hexahydrate ($FeCl_3{\cdot}6H_2O$), calcium chloride ($CaCl_2$), 3,3′,5,5′-tetramethylbenzidine (TMB), hydrogen peroxide (H_2O_2), sodium acetate, C-reactive protein (CRP), 4,4′-azobis(4-cyanovaleric acid) (ACVA), 4-cyanopentanoic acid dithiobenzoate (CPD), phosphate buffered saline pH 7.4 (PBS), and dialysis bag (cutoff molecular weight of 3500 g/mol) were purchased from Sigma-Aldrich (USA). Ammonium hydroxide solution (NH_4OH, 28% w/v), ethanol (EtOH), and acetic acid were purchased from Merck (Germany). All reagents and materials are of analytical grade and used without further purification. Ultrapure distilled water was obtained after purification using a Millipore Milli-Q system (USA) involving reverse osmosis, ion exchange, and filtration. The rabbit serum was purchased from Invitrogen.

2.2. Instrumentation. PMAMPC was characterized by nuclear magnetic resonance spectroscopy (NMR) in D_2O using a JEOL JNM-ECZ500R/S1 instrument (500 MHz). Percentage of conversion, composition of MA and MPC, and degree of polymerization (DP) can be calculated from relative peak integration by MestReNova program. Attenuated total reflectance-Fourier transform infrared (ATR-FTIR) spectra were recorded with an FTIR spectrometer (Thermo Scientific, Nicolet 6700, USA), model Impact 410, with 32 scans at resolution 4 cm^{-1}. A frequency range of 4000−500 cm^{-1} was collected by using a TGS detector. Thermogravimetric analysis (TGA) was carried out employing a Diamond TG/DTA (NETZSCH TG 209F3, Germany), and tests were operated under a dynamic nitrogen atmosphere flowing in a temperature range of 30−800 °C and the heating rate was set at 10 °C/min. The morphology and actual size of particles were evaluated using a transmission electron microscope (TEM, Philips TECNAI 20, U.K.) operated at 200 kV equipped with a 3CCD camera. A sample solution (0.2 mg/mL) in Milli-Q water was directly cast onto carbon-coated copper grids and dried in a desiccator before analysis. The Semafore software was used to determine the average diameters from 50 random particles for each sample. The phase structures of MNPs were characterized by powder X-ray diffraction (XRD, Rigaku, SmartLab 30 kV) with Cu Kα radiation (λ = 1.5418 Å). The measurements were recorded by monitoring the diffraction pattern appearing in the 2θ range from 20 to 70°. The particle size and ζ potential of the MNPs were measured by dynamic light scattering (DLS). The MNPs suspensions were diluted in Milli-Q water and placed into a cuvette. The measurements were taken at 25 °C three times for each sample using Zetasizer (Malvern Nano ZSP, U.K.) to determine the average

https://doi.org/10.1021/acsomega.4c10064
ACS Omega 2025, 10, 10317−10326

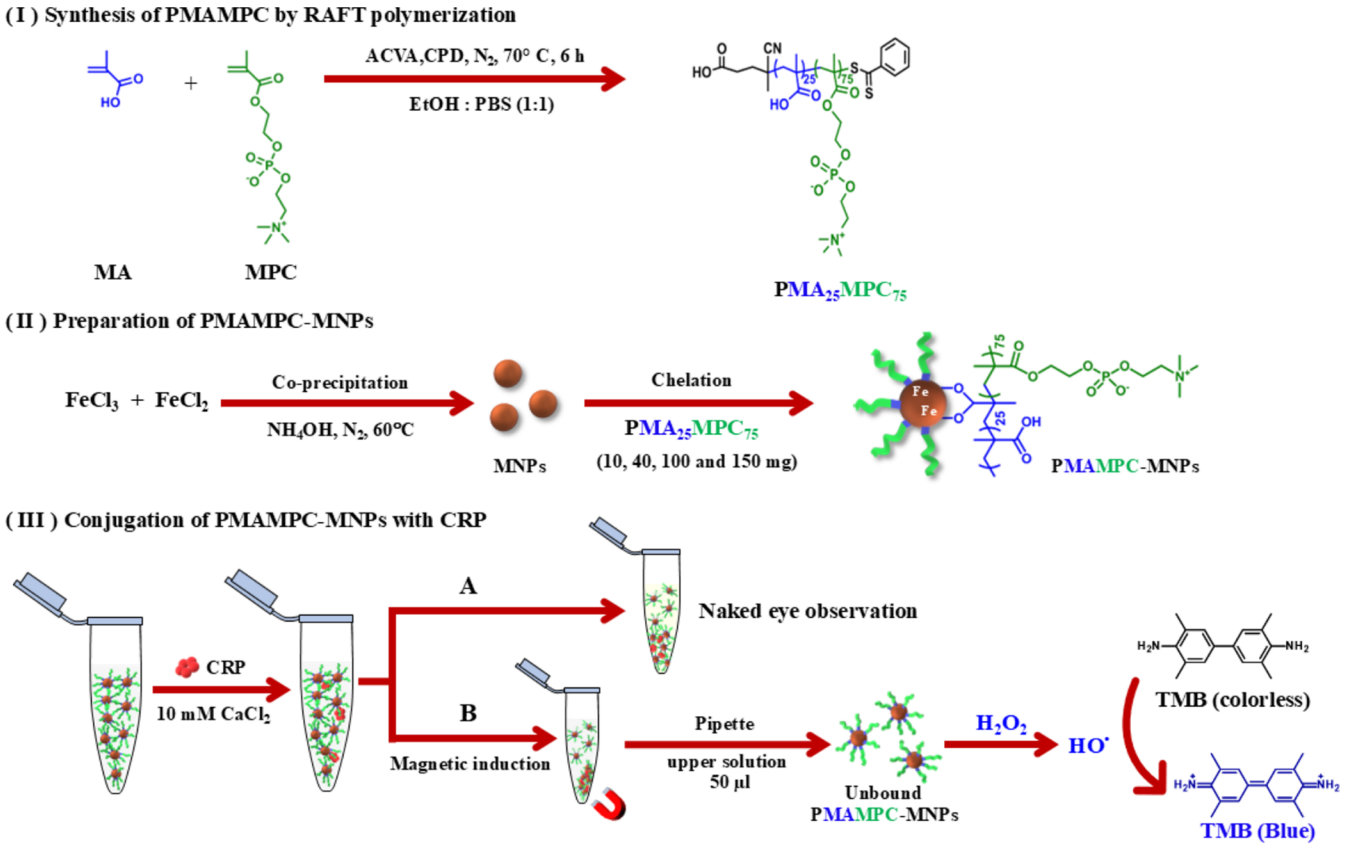

Figure 1. (I) Synthesis of PMAMPC, (II) preparation of PMAMPC-MNPs, and (III) conjugation of PMAMPC-MNPs with CRP, and the amount of CRP was observed by (A) naked eye and (B) magnetic induction followed by colorimetric method.

size distribution and *z*-average diameter. ζ-Potential measurements of these MNP suspensions were also determined using the same instrument. The suspensions were diluted with Milli-Q water and added into ζ-cell, and measurements were taken three times for each sample at 25 °C. UV−vis absorbance measurements of the MNPs suspensions after oxidation with TMB/H_2O_2 solution after 20 min incubation in 96 microplates were done by a UV−vis spectrophotometer (SpectraMax M2e microplate Reader, Molecular Devices). The experiment was shown in absorbance spectra of a compound in solution.

2.3. Synthesis of PMAMPC and PMAMPC-Functionalized MNPs. PMAMPC having a targeted degree of polymerization (DP) of 100 and the comonomer composition (MA/MPC) of 30:70 was synthesized by reversible addition−fragmentation chain transfer (RAFT) polymerization following a published procedure,[22] as shown in Figure 1I. Detailed experiment and determination of %conversion, degree of polymerization, and copolymer composition are provided in the Supporting Information. The polymer was purified and characterized by IR spectroscopy and ^{1}H NMR spectroscopy. After that, PMAMPC-functionalized MNPs were synthesized by two-step coprecipitation[22] as shown in Figure 1II. The detailed experiment is also provided in the Supporting Information. In the coprecipitation step, a desired amount of PMAMPC (10, 40, 100, and 150 mg) was added to the solution mixture and stirred for 60 min to allow chelation between carboxylic groups of PMAMPC and Fe atom on the surface of MNPs. The colloidal solution of PMAMPC-MNPs was freeze-dried and characterized by ATR-FTIR spectroscopy, TEM, DLS, TGA spectroscopy, and XRD.

2.4. Colloidal Stability of PMAMPC-MNPs. A suspension of PMAMPC-MNPs (0.6 mL, 1.0 mg/mL) prepared using different amounts of PMAMPC (10, 40, 100, and 150 mg) was diluted with deionized water (DW) to get a total volume of 3 mL. Colloidal stability of the PMAMPC-MNPs suspension was monitored by naked eye observation for 15 min and more than 60 min. The tests were also performed in the presence of calcium chloride ($CaCl_2$) at a time interval of 30 and 60 min. Varied concentrations of $CaCl_2$ (1, 2, and 3 mM) were added into PMAMPC-MNPs (0.4 mg/mL).

2.5. Conjugation of PMAMPC-MNPs with CRP. An appropriate amount of PMAMPC-MNPs that can conjugate with CRP and induce particle precipitation in a timely fashion was first identified, as shown in Figure 1IIIA. A varied volume (10, 20, 30, and 40 μL) of PMAMPC-MNPs in aqueous suspension (1 mg/mL) was added with DW to adjust the total volume to 90 μL and followed by an addition of 10 mM $CaCl_2$ (10 μL). The particle precipitation was observed by the naked eye at 0, 20, 40, and 60 min in the presence of 20 μg/mL CRP. A predetermined volume (1.25, 2.5, 5, 10, 15, and 20 μL) of 100 μg/mL CRP in 0.01 M PBS buffer was added into 1.0 mg/mL PMAMPC-MNPs aqueous suspension of which its optimal quantity was identified above. 10 μL of 10 mM $CaCl_2$ was then introduced, and the total volume of the solution was adjusted to 100 μL. Precipitation of PMAMPC-MNPs in the presence of varied amounts of CRP was monitored as a function of time without an external magnetic field. To determine the specificity of the PMAMPC-MNPs for CRP detection, the same protocol was applied for human serum albumin (HSA) and γ-globulin (20 μg/mL).

https://doi.org/10.1021/acsomega.4c10064
ACS Omega 2025, 10, 10317−10326

2.6. Colorimetric Detection of CRP Using PMAMPC-MNPs with TMB/H_2O_2. PMAMPC-MNPs (40 μL, 1 mg/mL), a varied volume (1, 2, 3, 4, and 5 μL) of 100 μg/mL CRP in 0.01 M PBS buffer (pH 7.4), and $CaCl_2$ (10 μL, 10 mM) were added to a 1.5 mL Eppendorf tube. The total volume was adjusted to 100 μL with DI-water, vortex-mixed, and then incubated for 5 min to allow conjugation between PMAMPC-MNPs and CRP. A magnet was then applied under the tube for 30 s to induce precipitation. 50 μL of supernatant containing unbound PMAMPC-MNPs was taken from the tube and added into each well of a 96-well microplate containing 197 μL of 0.1 M acetate buffer (pH 3.8). H_2O_2 (1.53 μL, 9.8 M) was then added, followed by TMB (0.5 μL, 100 mM) solution in dimethyl sulfoxide (DMSO) to obtain a final volume of 250 μL with DI-water. The 96-well microplate was shaken on the shaker and incubated at room temperature for 20 min. The absorbance of the solution in the 96-well microplate was measured at 650 nm using a UV−vis spectrophotometer (SpectraMax M2/M2e microplate reader). The amount of unbound PMAMPC-MNPs can be calculated from a calibration curve generated from PMAMPC-MNPs of known concentration in a range of 0−5 μg/mL CRP. The amount of unbound PMAMPC-MNPs is inversely proportional to the amount of CRP as shown in Figure 1IIIB.

3. RESULTS AND DISCUSSION

3.1. Synthesis of PMAMPC-Functionalized MNPs. PMAMPC-MNPs were prepared by the two-step coprecipitation following the published procedure[22] as shown in Figure 1I,II. The surface modification of MNPs with PMAMPC was verified by ATR-FTIR. As displayed in Figure 2, a characteristic Fe−O vibration of the unmodified MNPs was observed at 550 cm^{-1} in both unmodified MNPs (a) and PMAMPC-MNPs (b−f). Bands at 953, 1053, and 1715 cm^{-1}, assignable to $N^+(CH_3)_3$, P−O, and C═O stretching, respectively, apparently emerged in the spectra of PMAMPC-MNPs prepared by using 100 and 150 mg of PMAMPC (d and e) which coincided with PMAMPC (f). Such peaks were absent in the spectra of PMAMPC-MNPs prepared by using 10 and 40 mg of PMAMPC (b and c). This may be explained as a result of the PMAMPC of 40 mg, which is too low to be detectable by ATR-FTIR.

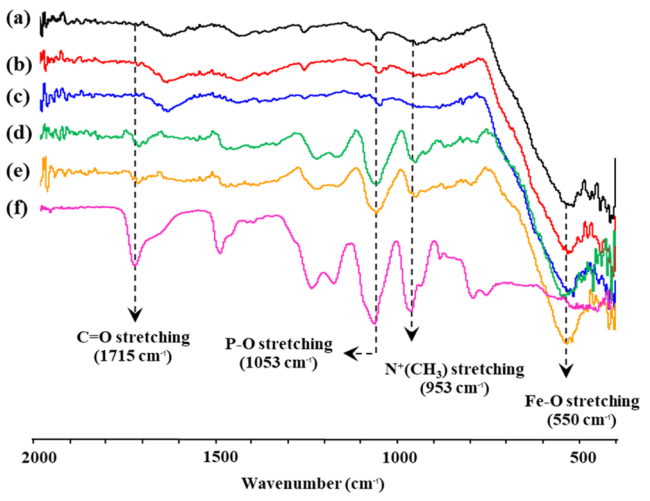

Figure 2. ATR-IR spectra of (a) bare MNPs and PMAPMC-MNPs prepared by using PMAMPC of (b) 10, (c) 40, (d) 100, and (e) 150 mg and (f) PMAMPC.

The crystallographic structure and composition of the PMAMPC-MNPs were identified by XRD, the patterns of which are shown in Figure S2, Supporting Information. The diffraction peaks of bare MNPs appeared at 30.04° (220), 35.33° (311), 43.06° (400), 53.51° (422), 57.09° (511), and 62.71° (440), which were consistent with the literature values of standard Fe_3O_4 crystals with inverse spinel structure.[33,34] Apparently, the PMAMPC coating did not have a noticeable impact on the MNPs crystallographic structure.[35]

The TGA curves of the PMAMPC-MNPs in comparison with bared MNPs are shown in Figure S3, Supporting Information. The first weight loss of all MNPs took place at about 100 °C as a result of dehydration. PMAMPC-MNPs prepared by using PMAMPC of 40 mg showed the highest weight loss of about 2.8%, implying that they contained the greatest bound water content. The second weight loss occurring in a temperature range of 200−400 °C could be ascribed to the decomposition of PMAMPC bonded to MNPs.[22,36,37] The greater weight loss of 7.6 and 7.9% of PMAPMC-MNPs prepared by using 100 and 150 mg, respectively, than that of bare MNPs (2.1%), PMAPMC-MNPs prepared by using 10 (2.2%) and 40 (2.8%) mg confirmed the presence of varied amount PMAMPC on MNPs. The third weight loss appeared at the highest temperature (>730 °C) for the PMAMPC-MNPs prepared by using 100 and 150 mg. This should be a contribution of char of macromolecular organic content (PMAMPC) on the PMAMPC-MNPs because such weight loss was absent in the curves of bared MNPs and PMAMPC-MNPs prepared by using low quantity of PMAMPC (10 and 40 mg).

The results from the investigation of the stability of PMAMPC-MNPs over time, shown in Figure S4 in the Supporting Information, match the findings from the ATR-FTIR analysis. It was found that using 10 and 40 mg of PMAMPC was insufficient to produce stable PMAMPC-MNPs, as they precipitated after just 15 min, much like the uncoated MNPs. However, when 100 mg of PMAMPC was used, the PMAMPC-MNPs remained stable for over an hour, indicating that this amount was sufficient to stabilize the MNPs and prevent precipitation. However, increasing the PMAMPC to 150 mg resulted in PMAMPC-MNPs with reduced dispersibility, causing precipitation after 60 min. Therefore, the PMAMPC-MNPs prepared using 100 mg of PMAMPC were selected for further study.

3.2. Conjugation of PMAMPC-MNPs with CRP. Various concentrations of $CaCl_2$ in a range of 1−3 mM were added into 0.4 mg/mL PMAMPC-MNPs aqueous suspension. As shown in Figure 3A, the PMAMPC-MNPs solution had good colloidal stability in the presence of $CaCl_2$ of 1 and 2 mM for up to 60 min. Precipitation of the PMAMPC-MNPs (0.4 mg/mL) prepared using 100 mg of PMAMPC was observed when the $CaCl_2$ concentration reached 3 mM at 60 min. To minimize the risk of Ca^{2+}-induced precipitation of the PMAMPC-MNPs even without CRP, 1 mM $CaCl_2$ was chosen for CRP detection.

Specific binding of CRP (20 μg/mL) was tested with PMAMPC-MNPs of varied concentrations (0.1, 0.2, 0.3, and 0.4 mg/mL) in the presence of 1 mM $CaCl_2$. As shown in Figure 3B, no sedimentation of 0.1 mg/mL PMAMPC-MNPs was observed, even in the presence of CRP, suggesting that the PMAMPC-MNPs concentration was too low. The addition of

https://doi.org/10.1021/acsomega.4c10064
ACS Omega 2025, 10, 10317−10326

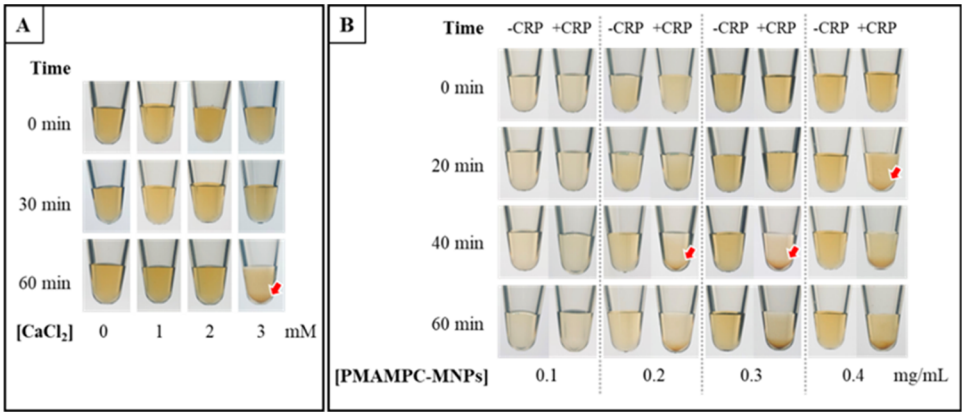

Figure 3. Appearance of colloidal (A) PMAMPC-MNPs (0.4 mg/mL) in the presence of varied $CaCl_2$ concentration as a function of incubation time and (B) PMAMPC-MNPs of varied concentration before and after the addition of CRP (20 μg/mL) in the presence of 1 mM $CaCl_2$ as a function of incubation time.

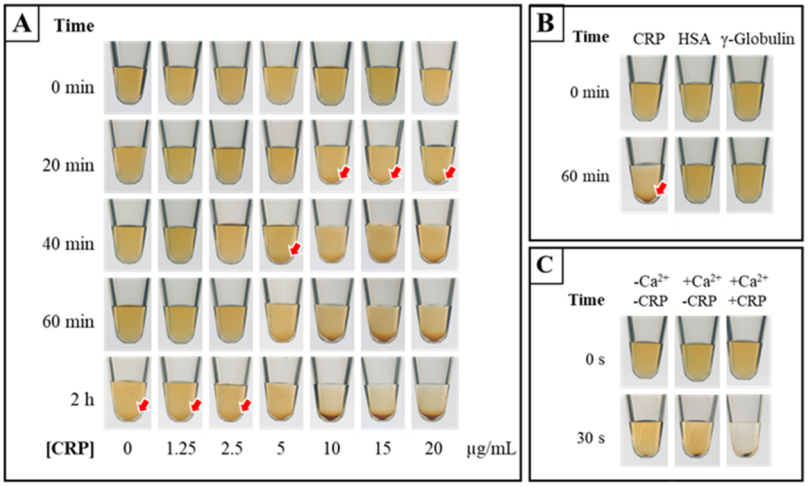

Figure 4. Appearance of colloidal PMAMPC-MNPs upon (A) addition of varied CRP concentration as a function of time, (B) CRP in comparison with HSA and γ-globulin with Ca^{2+}, and (C) Ca^{2+} together with CRP under the external magnetic field.

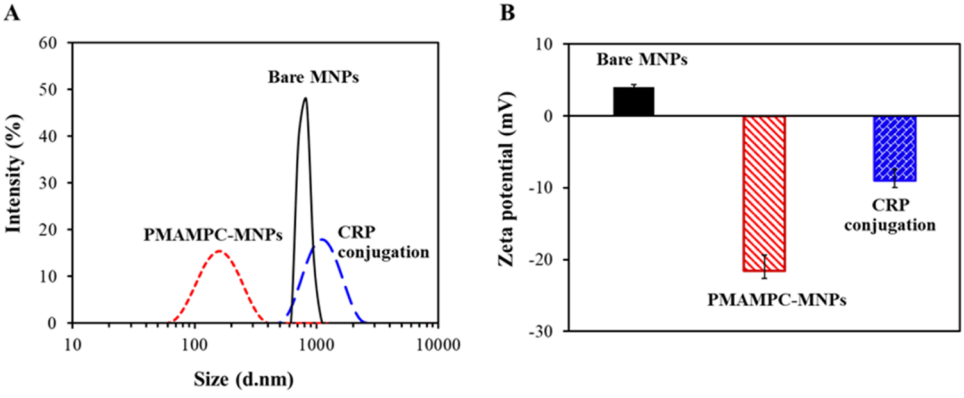

Figure 5. (A) DLS profiles and (B) ζ-potential values of bare MNPs and PMAMPC-MNPs both before and after the addition of CRP (5 μg/mL) in the presence of 1 mM Ca^{2+}.

CRP, which can bind to PMAMPC-MNPs, induced precipitation of 0.2 and 0.3 mg/mL PMAMPC-MNPs after incubation for 40 min of incubation. The CRP-induced precipitation of 0.4 mg/mL PMAMPC-MNPs occurred after a shorter incubation period (20 min). Therefore, a concentration of 0.4 mg/mL was chosen as an optimal PMAMPC-MNPs concentration for CRP detection.

Upon using 1 mM $CaCl_2$ and 0.40 mg/mL PMAMPC-MNPs, the conjugation of PMAMPC-MNPs with varied concentrations of CRP, which can induce precipitation without the application of an external magnetic field, was investigated as a function of time. The results shown in Figure 4A demonstrate that the precipitation occurred more rapidly in the presence of 10 μg/mL CRP or higher compared to lower

https://doi.org/10.1021/acsomega.4c10064
ACS Omega 2025, 10, 10317−10326

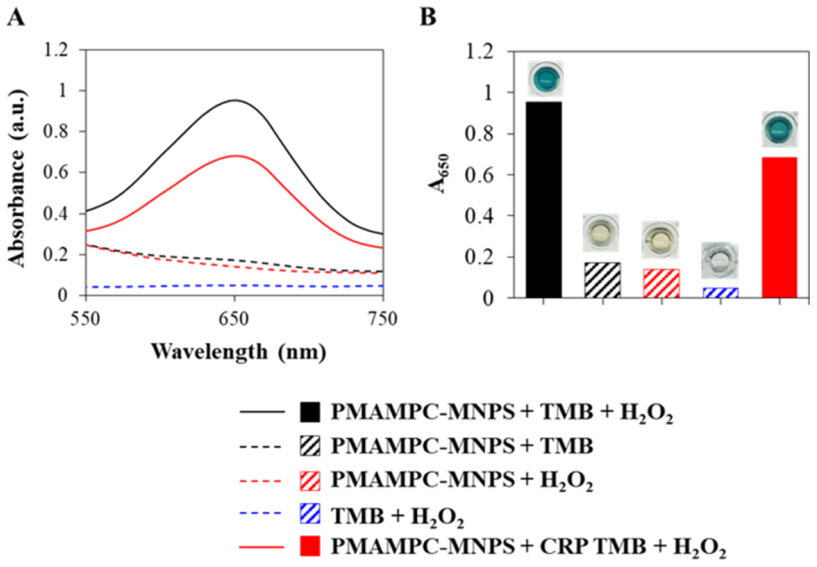

Figure 6. UV−vis absorption (A) spectra and (B) bar graphs of UV−vis absorbance at 650 nm of PMAMPC-MNPs + TMB + H_2O_2 (black solid line and black filled strip), PMAMPC-MNPs + TMB (black dashed line and black pattern), PMAMPC-MNPs + H_2O_2 (red dashed line and red pattern), TMB + H_2O_2 (blue dashed line and blue pattern), and PMAMPC-MNPs + CRP + TMB + H_2O_2 (red solid line and red filled strip). The insets in (B) show the appearance of solution in the well plates.

CRP concentrations. The minimum concentration of CRP that could induce precipitation within a reasonable period (40 min) was 5 μg/mL. The conjugation was also performed with human serum albumin (HSA) and γ-globulin for comparison. As illustrated in Figure 4B, precipitation was not observed upon the addition of HSA and γ-globulin as opposed to CRP, suggesting the specificity of PMAMPC-MNPs toward CRP and verifying antifouling characteristic of the PMAMPC against other nonspecific proteins. The effect of the external magnetic field on the CRP conjugation on PMAMPC-MNPs was also investigated. The results shown in Figure 4C indicated that the precipitation of PMAMPC-MNPs in the presence of Ca^{2+} and CRP was accelerated by the external magnetic field, occurring within 30 s (right tube). In the absence of CRP (middle tube), only a small amount of PMAMPC-MNPs was found to precipitate.

The hydrodynamic diameter and ζ-potential of PMAMPC-MNPs were determined by DLS. As shown in Figure 5A, the hydrodynamic radius of the bare MNPs was 796 ± 182 nm. These data strongly indicate that aqueous dispersibility of the bared MNPs was poor, so extensive agglomeration was observed. The diameter of PMAMPC-MNPs decreased to 140.5 ± 3.6 nm (polydispersity index (PDI) = 0.208). This much smaller hydrodynamic dimension suggested that PMAMPC was an effective stabilizing agent that could provide both steric stabilization and charge repulsion from the negatively charged carboxyl groups of MA units in the copolymer. The latter effect can be verified from the more negative ζ-potential value of the PMAMPC-MNPs (−21.6 ± 2.21 mV) as opposed to the bared MNPs (3.99 ± 0.34 mV). Upon conjugation with CRP, the hydrodynamic size of PMAMPC-MNPs became larger to 934.4 ± 82.1 nm (PDI = 0.260) as a result of agglomeration. The particle size would increase with increasing the CRP concentration and the linearity correlation was observed in the range of 0−5 μg/mL CRP (Figure S5, Supporting Information). The isoelectric point of CRP is approximately 6.3,[38] which causes CRP to become positively charged in DW (pH 5.5−6.5). Consequently, the ζ-potential of the PMAMPC-MNPs became less negative after CRP conjugation (−8.96 ± 1.52 mV; Figure 5B).

The morphology of bare MNPs and PMAPMC-MNPs both before and after conjugation with CRP was determined by TEM. The bare MNPs (Figure S6a, Supporting Information) showed a certain degree of agglomeration due to their poor aqueous dispersity. An average diameter of individual particles of 9.56 ± 1.63 nm was calculated. Less aggregation was observed for PMAPMC-MNPs, the diameter of which became slightly larger to 12.81 ± 2.71 nm as a result of the PMAPMC coating (Figure S6b, Supporting Information). After conjugating with CRP, extensive agglomeration was also realized. This may be ascribable to the conjugation with a relatively large molecule of CRP (115 kDa).[12,39] The average diameter of individual PMAPMC-MNPs was unaffected by CRP conjugation (Figure S6c in the Supporting Information). Results from TEM analysis apparently agree very well with the data obtained from DLS analysis.

3.3. Colorimetric Detection of CRP Using PMAMPC-MNPs with TMB/H_2O_2. The peroxidase catalytic activity behavior was examined through the oxidation of TMB in the presence of H_2O_2, catalyzed by PMAMPC-MNPs. The peroxidase-like activity was measured by monitoring a blue color of oxidized TMB, where the color intensity was directly proportional to the catalytic activity, which varied based on the quantity of the PMAMPC-MNPs. As shown in Figure 6, PMAMPC-MNPs catalyzed the oxidation of the TMB substrate, producing a blue solution detectable by UV−vis spectroscopy at 650 nm but only in the presence of both TMB and H_2O_2 (black solid line and black filled strip). With either TMB or H_2O_2 alone, the blue solution did not develop, implying that catalytic oxidation did not occur (black dashed line, black pattern, red dashed line, and red pattern). There was also no background color from a combination of TMB and H_2O_2 (blue dashed line and blue pattern), suggesting that the development of the blue-colored solution occurred as a result of the peroxidase-like activity of PMAMPC-MNPs in the

https://doi.org/10.1021/acsomega.4c10064
ACS Omega 2025, 10, 10317−10326

presence of TMB and H_2O_2. As shown in Figure 1IIIB, after CRP conjugation, part of CRP-PMAMPC-MNPs complexes precipitated with magnetic induction, and only unbound PMAMPC-MNPs remaining in the supernatant exhibited peroxidase-like activity. As a result, the intensity of the developed, blue-colored solution was lower (red solid line and red filled strip) compared to that of the PMAMPC-MNPs before CRP conjugation (black solid line and black filled strip).

The conjugation of PMAMPC-MNPs with varied CRP concentration in a range of 0−5 μg/mL was evaluated. Figure 7A shows the intensity of the blue solution produced by

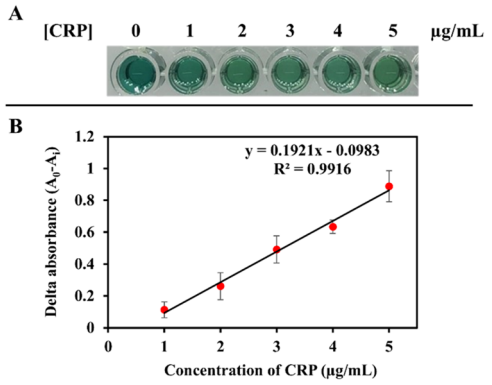

Figure 7. (A) Appearance of the solution and (B) calibration plot of delta-UV−vis absorbance as a function of CRP concentration and the solution of unbound PMAMPC-MNPs after oxidation with TMB and H_2O_2.

unbound PMAMPC-MNPs in the supernatant after the PMAMPC-MNPs were conjugated with CRP. The intensity of the blue solution was found to decrease as the CRP concentration increased. The deltaabsorbance ($A_0 - A_I$) exhibited a linear range of 1−5 μg/mL (Figure 7B), with a linear equation of $y = 0.192x - 0.0983$ ($R^2 = 0.9916$). The experimental limit of detection (LOD), defined as the lowest detectable CRP concentration providing a signal distinguishable from the blank (0 μg/mL), was found to be 1.0 μg/mL.

3.4. Analysis of CRP in Rabbit Serum Samples. The performance of the PMAMPC-MNPs was further evaluated for the analysis of CRP in the added rabbit serum samples. The validation procedure was performed by adding 3.0 μg/mL CRP in 0% (aqueous solution), 50% diluted, and undiluted rabbit serum solutions. It was found that the intensity of the blue-colored solution produced by the unbound PMAMPC-MNPs without CRP conjugation in 50% diluted and undiluted rabbit serum solutions (100%) was found to be lower than that in 0% serum (Figure S7, Supporting Information). This may be explained by the fact that proteins in the rabbit serum deteriorated the catalytic activity of the PMAMPC-MNPs to some extent. However, after CRP conjugation, the intensity of the blue solution proportionally decreased as anticipated. The delta absorbance intensity is 0.4431, 0.3810, and 0.3364 for 0, 50% diluted, and undiluted rabbit serum solutions, respectively (Figure S7, Supporting Information). The measured CRP amounts were 2.82 ± 0.01 μg/mL (93.9% recovery), 2.49 ± 0.18 μg/mL (82.2% recovery), and 2.26 ± 0.27 μg/mL (75.4% recovery) in 0, 50% diluted, and undiluted rabbit serum solutions, respectively (Tabel 1). The recovery test of the added samples in 0 and 50% diluted rabbit serum was found to be within the recommended recovery range (80−110%) by the

Table 1. Results of Determination of CRP in Added Rabbit Serum Samples

no	samples	added CRP (μg/mL)	measured ± SD (n = 3)	recovery (%)
1	0% rabbit serum	0.0	ND[a]	
		3.0	2.82 ± 0.01	93.9 ± 0.2
2	50% rabbit serum	0.0	ND	
		3.0	2.49 ± 0.18	83.2 ± 6.2
3	undiluted rabbit serum	0.0	ND	
		3.0	2.26 ± 0.27	75.4 ± 9.1

[a]ND = not detected.

AOAC at analyte concentration levels of 3.0 μg/mL.[40] The results indicated that PMAMPC-MNPs are suitable for the analysis of CRP in complex matrix samples.

The comparison of the analytical performance between this sensor and other sensors is presented in Table 2. In general, antibody-based sensors (entries 3−6) offer high specificity as well as sensitivity with LODs in the ng/mL range. However, using antibodies is quite costly and has limited stability. Phosphorylcholine (PC) groups have been introduced as an efficient, nonantibody alternative. By employing PC-bovine serum albumin (BSA)-conjugated carboxylate microspheres, detection via turbidimetric and ELISA assay (entries 1 and 2) provided a linear range of 0.5−10 and 0−10 mg/mL, respectively. PMPC having multiple PC groups along the chain was also applied as probes for CRP detection (entries 7−9). As anticipated, electrochemical detection using differential pulse voltammetry (DPV) offers the lowest LOD (1.55×10^{-3} μg/mL) in comparison with localized surface plasmon resonance (LSPR) and dynamic light scattering (DLS). However, the risk value for cardiovascular disease falls in the linear ranges obtained for all techniques (DPV, LSPR, and DLS).

From this study, it can be seen that the use of colorimetric assay based on PMAMPC-MNPs exhibits equivalent performance in terms of LOD (1.0 μg/mL) to ELISA assay based on PC-BSA-conjugated carboxylated microspheres and a linear range of detection similar to those based on PC-BSA-conjugated carboxylated microspheres via turbidimetric and ELISA assay (entries 1 and 2). In comparison with other assays employing MNPs, the PMAMPC-MNPs are superior to polyclonal goat anti-CRP (covalently) bound MNPs (entry 5) since they are antibody-free and also provide a broader linear range of CRP detection. The colorimetric assay based on PMAMPC-MNPs showed a similar LOD to that of PMPC-Fe_3O_4-based DLS analysis (1.15 μg/mL) (entry 8). Nevertheless, the preparation for PMAMPC-MNPs by the two-step coprecipitation is much simpler and less sophisticated than the method used for PMPC-Fe_3O_4, which involves coprecipitation followed by surface-initiated polymerization. Besides, the colorimetric method can be easily implemented for on-site detection, unlike DLS analysis, which requires specialized instruments.

4. CONCLUSIONS

The PMAMPC-MNPs have been successfully prepared through the two-step coprecipitation. The PMAMPC coating did not affect the MNP crystal structure, and PMAMPC-MNPs were found to be colloidally stable. A colloidal stability test suggested that the PMAMPC-MNPs prepared using 100

https://doi.org/10.1021/acsomega.4c10064
ACS Omega 2025, 10, 10317−10326

Table 2. Analytical Characteristics of Different CRP Biosensors Previously Reported

	entry	assay type	materials/substrate	linear range (μg/mL)	LOD (μg/mL)	reference
PC-based	1	turbidimetric method	PC-BSA-conjugated carboxylated microspheres	0.5−10		Deegan et al.[41]
	2	enzyme-linked absorbance assay (ELISA)	PC-BSA-conjugated carboxylated microspheres	0−10	1.06	Deegan et al.[41]
antibody-based	3	immunoassay (agglutination)	anti-CRP (monoclonal antibody)-immobilized MPC-PNPs	1−1000		Park et al.[18]
	4	nephelometric method	anti-CRP-bound polystyrene bead and acridinium-labeled anti-CRP	0.01−50	4.0×10^{-3}	Shiesh et al.[42]
	5	immunomagnetic reduction (IMR)	polyclonal goat anti-CRP (covalently)-bound MNPs	0.1−1		Chang et al.[43]
	6	sandwich nanoparticle immunoassay	anti-CRP-modified iron oxide@SiO_2 and (CdSe/ZnS)@SiO_2	0.00118−11.8	1.0×10^{-3}	Yang et al.[44]
PC polymer-based	7	localized surface plasmon resonance (LSPR)	PMPC-*b*-PMAT-SH-modified AuNPs	0−9.5	2.3−4.7	Iwasaki et al.[20]
	8	dynamic light scattering (DLS)	PMPC-Fe_3O_4	0−69	1.15	Iwasaki et al.[21]
	9	differential pulse voltammetry (DPV)	PMPC-SH-modified AuNPs-SPCE/PADs	0.005−5	1.55×10^{-3}	Pinyorospathum et al.[19]
	10	flocculation method (necked eye)	PMAMPC-MNPs	5−20	5.0	this work
		colorimetric method		1−5	1.0	

mg of PMAMPC were the most suitable particles for further studies, as they remained stable for up to 1 month. In the presence of Ca^{2+}, no precipitation was observed upon the addition of HSA and γ-globulin, unlike with CRP, suggesting the specificity of PMAMPC-MNPs toward CRP and confirming the antifouling properties of PMAMPC against other nonspecific proteins. This specific conjugation of CRP and PMAMPC-MNPs was confirmed through DLS and TEM analysis. Therefore, PMAMPC-MNPs were used to detect CRP via naked eye observation and a colorimetric assay using TMB as a substrate, along with H_2O_2. The intensity of the blue-colored solution decreased linearly as a function of CRP within a concentration range of 1−5 μg/mL, with an experimental LOD of 1.0 μg/mL. Finally, this method can detect 3 μg/mL (risk value of cardiovascular disease) in 50% diluted rabbit serum.

■ ASSOCIATED CONTENT

Supporting Information

The Supporting Information is available free of charge at https://pubs.acs.org/doi/10.1021/acsomega.4c10064.

Synthesis and characterization of PMAMPC and PMAMPC-functionalized MNPs, ^{1}H NMR spectra, XRD spectra, TGA curves, appearance of aqueous dispersion, TEM micrographs, DLS profiles, and absorbance of blue-colored solution (PDF)

■ AUTHOR INFORMATION

Corresponding Author

Piyaporn Na Nongkhai − *Research Unit for Sensor Innovation (RUSI) and Department of Chemistry and Center of Excellence for Innovation in Chemistry, Faculty of Science, Burapha University, Chon Buri 20131, Thailand;* orcid.org/0000-0001-9358-6853; Email: piyapornn@buu.ac.th

Authors

Tinnakorn Phuangkaew − *Department of Chemistry, Faculty of Science, Chulalongkorn University, Bangkok 10330, Thailand;* orcid.org/0000-0002-5942-7223

Suttawan Saipai − *Program in Petrochemistry and Polymer Science, Faculty of Science, Chulalongkorn University, Bangkok 10330, Thailand*

Voravee P. Hoven − *Department of Chemistry, Faculty of Science and Center of Excellence in Materials and Bio-interfaces, Chulalongkorn University, Bangkok 10330, Thailand;* orcid.org/0000-0002-1330-6784

Complete contact information is available at: https://pubs.acs.org/10.1021/acsomega.4c10064

Notes

The authors declare no competing financial interest.

■ ACKNOWLEDGMENTS

This research was supported by Thailand Science Research and Innovation Fund Chulalongkorn University and the Center of Excellence for Innovation in Chemistry (PERCH-CIC), Burapha University.

■ REFERENCES

(1) Kaptoge, S.; Pennells, L.; De Bacquer, D.; Cooney, M. T.; Kavousi, M.; Stevens, G.; Riley, L. M.; Savin, S.; Khan, T.; Altay, S.; et al. World Health Organization Cardiovascular Disease Risk Charts: Revised Models to Estimate Risk in 21 Global Regions. *Lancet Global Health* **2019**, *7* (10), e1332−e1345.

(2) Upadhyay, R. K. Emerging Risk Biomarkers in Cardiovascular Diseases and Disorders. *J. Lipids* **2015**, *2015*, No. 971453.

(3) Pearson, T. A.; Mensah, G. A.; Alexander, R. W.; Anderson, J. L.; Cannon, R. O., 3rd; Criqui, M.; Fadl, Y. Y.; Fortmann, S. P.; Hong, Y.; Myers, G. L.; et al. Markers of Inflammation and Cardiovascular Disease: Application to Clinical and Public Health Practice: A Statement for Healthcare Professionals from the Centers for Disease Control and Prevention and the American Heart Association. *Circulation* **2003**, *107* (3), 499−511.

(4) Ridker, P. M. C-Reactive Protein. *Circulation* **2003**, *108* (12), e81−e85.

(5) Mali, B.; Armbruster, D.; Serediak, E.; Ottenbreit, T. Comparison of Immunoturbidimetric and Immunonephelometric Assays for Specific Proteins. *Clin. Biochem.* **2009**, *42* (15), 1568−1571.
(6) Drieghe, S. A.; Alsaadi, H.; Tugirimana, P. L.; Delanghe, J. R. A New High-Sensitive Nephelometric Method for Assaying Serum C-Reactive Protein Based on Phosphocholine Interaction. *Clin. Chem. Lab. Med.* **2014**, *52* (6), 861−867.
(7) Tugirimana, P. L.; De Clercq, D.; Holderbeke, A. L.; Kint, J. A.; De Cooman, L.; Deprez, P.; Delanghe, J. R. A Functional Turbidimetric Method to Determine C-Reactive Protein in Horses. *J. Vet. Diagn. Invest.* **2011**, *23* (2), 308−311.
(8) Correia, L. C. L.; Lima, J. C.; Gerstenblith, G.; Magalhães, L. P.; Moreira, A.; Jr, B.; Octávio, D. J.; Passos, L. C. S.; D'Oliveira, J. A.; Esteves, J. P. Correlation between Turbidimetric and Nephelometric Methods of Measuring C-Reactive Protein in Patients with Unstable Angina or Non-ST Elevation Acute Myocardial Infarction. *Arq. Bras. Cardiol.* **2003**, *81* (2), 133−136.
(9) Fakanya, W. M.; Tothill, I. E. Detection of the Inflammation Biomarker C-Reactive Protein in Serum Samples: Towards an Optimal Biosensor Formula. *Biosensors* **2014**, *4* (4), 340−357.
(10) Letchumanan, I.; Md Arshad, M. K.; Balakrishnan, S. R.; Gopinath, S. C. B. Gold-nanorod Enhances Dielectric Voltammetry Detection of C-reactive Protein: A Predictive Strategy for Cardiac Failure. *Biosens. Bioelectron.* **2019**, *130*, 40−47.
(11) Zhang, L.; Li, H. Y.; Li, W.; Shen, Z. Y.; Wang, Y. D.; Ji, S. R.; Wu, Y. An ELISA Assay for Quantifying Monomeric C-Reactive Protein in Plasma. *Front. Immunol.* **2018**, *9*, No. 511.
(12) Xu, J. P.; Ji, J.; Chen, W. D.; Shen, J. C. Novel Biomimetic Polymersomes as Polymer Therapeutics for Drug Delivery. *J. Controlled Release* **2005**, *107* (3), 502−512.
(13) Matsuno, R.; Ishihara, K. Integrated Functional Nanocolloids Covered with Artificial Cell Membranes for Biomedical Applications. *Nano Today* **2011**, *6* (1), 61−74.
(14) Ahmed, M.; Jawanda, M.; Ishihara, K.; Narain, R. Impact of the Nature, Size and Chain Topologies of Carbohydrate-Phosphorylcholine Polymeric Gene Delivery Systems. *Biomaterials* **2012**, *33* (31), 7858−7870.
(15) Yoshimoto, J.; Sangsuwan, A.; Osaka, I.; Yamashita, K.; Iwasaki, Y.; Inada, M.; Arakawa, R.; Kawasaki, H. Optical Properties of 2-Methacryloyloxyethyl Phosphorylcholine-Protected Au_4Nanoclusters and Their Fluorescence Sensing of C-Reactive Protein. *J. Phys. Chem. C* **2015**, *119* (25), 14319−14325.
(16) Wang, Q.; Jin, H.; Xia, D.; Shao, H.; Peng, K.; Liu, X.; Huang, H.; Zhang, Q.; Guo, J.; Wang, Y.; et al. Biomimetic Polymer-Based Method for Selective Capture of C-Reactive Protein in Biological Fluids. *ACS Appl. Mater. Interfaces* **2018**, *10* (49), 41999−42008.
(17) Kitayama, Y.; Takeuchi, T. Localized Surface Plasmon Resonance Nanosensing of C-Reactive Protein with Poly(2-Methacryloyloxyethyl Phosphorylcholine)-Grafted Gold Nanoparticles Prepared by Surface-Initiated Atom Transfer Radical Polymerization. *Anal. Chem.* **2014**, *86* (11), 5587−5594.
(18) Park, J.; Kurosawa, S.; Watanabe, J.; Ishihara, K. Evaluation of 2-Methacryloyloxyethyl Phosphorylcholine Polymeric Nanoparticle for Immunoassay of C-Reactive Protein Detection. *Anal. Chem.* **2004**, *76* (9), 2649−2655.
(19) Pinyorospathum, C.; Chaiyo, S.; Sae-Ung, P.; Hoven, V. P.; Damsongsang, P.; Siangproh, W.; Chailapakul, O. Disposable Paper-Based Electrochemical Sensor Using Thiol-Terminated Poly(2-Methacryloyloxyethyl Phosphorylcholine) for the Label-Free Detection of C-Reactive Protein. *Mikrochim. Acta* **2019**, *186* (7), No. 472.
(20) Iwasaki, Y.; Kimura, T.; Orisaka, M.; Kawasaki, H.; Goda, T.; Yusa, S. Label-Free Detection of C-Reactive Protein Using Highly Dispersible Gold Nanoparticles Synthesized by Reducible Biomimetic Block Copolymers. *Chem. Commun.* **2014**, *50* (42), 5656−5658.
(21) Iwasaki, S.; Kawasaki, H.; Iwasaki, Y. Label-Free Specific Detection and Collection of C-Reactive Protein Using Zwitterionic Phosphorylcholine-Polymer-Protected Magnetic Nanoparticles. *Langmuir* **2019**, *35* (5), 1749−1755.
(22) Boonjamnian, S.; Trakulsujaritchok, T.; Srisook, K.; Hoven, V. P.; Nongkhai, P. N. Biocompatible Zwitterionic Copolymer-Stabilized Magnetite Nanoparticles: a Simple One-Pot Synthesis, Antifouling Properties and Biomagnetic Separation. *RSC Adv.* **2018**, *8* (65), 37077−37084.
(23) Adeoye, A. O. M.; Kayode, J. F.; Oladapo, B. I.; Afolabi, S. O. Experimental Analysis and Optimization of Synthesized Magnetic Nanoparticles Coated with PMAMPC-MNPs for Bioengineering Application. *St. Petersburg Polytech. Univ. J.: Phys. Math.* **2017**, *3* (4), 333−338.
(24) Goda, T.; Tabata, M.; Sanjoh, M.; Uchimura, M.; Iwasaki, Y.; Miyahara, Y. Thiolated 2-Methacryloyloxyethyl Phosphorylcholine for an Antifouling Biosensor Platform. *Chem. Commun.* **2013**, *49* (77), 8683−8685.
(25) Chen, S. H.; Fukazawa, K.; Inoue, Y.; Ishihara, K. Photo-induced Surface Zwitterionization for Antifouling of Porous Polymer Substrates. *Langmuir* **2019**, *35* (5), 1312−1319.
(26) Sae-Ung, P.; Kolewe, K. W.; Bai, Y.; Rice, E. W.; Schiffman, J. D.; Emrick, T.; Hoven, V. P. Antifouling Stripes Prepared from Clickable Zwitterionic Copolymers. *Langmuir* **2017**, *33* (28), 7028−7035.
(27) Gao, L.; Wu, J.; Lyle, S.; Zehr, K.; Cao, L.; Gao, D. Magnetite Nanoparticlelinked Immunosorbent Assay. *J. Phys. Chem. C* **2008**, *112* (44), 17357−17361.
(28) Zhuang, J.; Zhang, J.; Gao, L.; Zhang, Y.; Gu, N.; Feng, J.; Yang, D.; Yan, X. A Novel Application of Iron Oxide Nanoparticles for Detection of Hydrogen Peroxide in Acid Rain. *Mater. Lett.* **2008**, *62* (24), 3972−3974.
(29) Le, T. N.; Tran, T. D.; Kim, M. I. A Convenient Colorimetric Bacteria Detection Method Utilizing Chitosan-Coated Magnetic Nanoparticles. *Nanomaterials* **2020**, *10* (1), No. 92.
(30) Wang, L.; Bai, H.; Liu, X.; Xiao, X.; Yu, Y.; Li, X. Colorimetric Sensor Based on Peroxidase-like Activity of Chitosan Coated on Magnetic Nanoparticles for Rapid Detection of the Total Bacterial Count in Raw Milk. *Eur. Food Res. Technol.* **2022**, *248* (5), 1321−1333.
(31) Kim, Y. S.; Jurng, J. A Simple Colorimetric Assay for the Detection of Metal Ions Based on the Peroxidase-like Activity of Magnetic Nanoparticles. *Sens. Actuators, B* **2013**, *176*, 253−257.
(32) Tian, L.; Zhao, B.; Zhang, J.; Luo, X.; Wu, F. Magnetic Covalent Organic Framework Nanospheres with Enhanced Peroxidase-like Activity for Colorimetric Detection of H_2O_2 and Glucose. *Colloids Surf., A* **2023**, *666*, No. 131309.
(33) Thanyasrisung, P.; Vittayaprasit, A.; Matangkasombut, O.; Sugai, M.; Na Nongkai, P.; Saipia, S.; Hoven, V. P. Separation and Detection of Mutans Streptococci by Using Magnetic Nanoparticles Stabilized with a Cell Wall Binding Domain-Conjugated Polymer. *Anal. Methods* **2018**, *10* (27), 3332−3339.
(34) Wei, Y.; Han, B.; Hu, X.; Lin, Y.; Wang, X.; Deng, X. Biomimetic Polymer-Based Method for Selective Capture of C-Reactive Protein in Biological Fluids. *Procedia Eng.* **2012**, *27*, 632−637.
(35) Jiang, W.; Wu, Y.; He, B.; Zeng, X.; Lai, K.; Gu, Z. Effect of Sodium Oleate as a Buffer on the Synthesis of Superparamagnetic Magnetite Colloids. *J. Colloid Interface Sci.* **2010**, *347* (1), 1−7.
(36) Vilela, C.; Moreirinha, C.; Almeida, A.; Silvestre, A. J. D.; Freire, C. S. R. Zwitterionic Nanocellulose-Based Membranes for Organic Dye Removal. *Materials* **2019**, *12* (9), No. 1404.
(37) Kaßel, M.; Gerke, J.; Ley, A.; Vana, P. Surface Modification of Wood Flour via ARGET ATRP and Its Application as Filler in Thermoplastics. *Polymers* **2018**, *10* (4), No. 354.
(38) Potempa, L. A.; Yao, Z. Y.; Ji, S. R.; Filep, J. G.; Wu, Y. Solubilization and Purification of Recombinant Modified C-Reactive Protein from Inclusion Bodies Using Reversible Anhydride Modification. *Biophys. Rep.* **2015**, *1*, 18−33.
(39) Meyer, M. H.; Hartmann, M.; Krause, H. J.; Blankenstein, G.; Mueller-Chorus, B.; Oster, J.; Miethe, P.; Keusgen, M. CRP Determination Based on a Novel Magnetic Biosensor. *Biosens. Bioelectron.* **2007**, *22* (6), 973−979.

https://doi.org/10.1021/acsomega.4c10064
ACS Omega 2025, 10, 10317−10326

(40) AOAC International. Appendix K: Guidelines for Dietary Supplements and Botanicals. *AOAC Official Methods of Analysis*; AOAC International, 2013; Vol. 2, pp 1−32.
(41) Deegan, O.; Walshe, K.; Kavanagh, K.; Doyle, S. Quantitative Detection of C-Reactive Protein Using Phosphocholine-Labelled Enzyme or Microspheres. *Anal. Biochem.* **2003**, *312* (2), 175−181.
(42) Shiesh, S. C.; Chou, T. C.; Lin, X. Z.; Kao, P. C. Determination of C-Reactive Protein with an Ultra-Sensitivity Immunochemiluminometric Assay. *J. Immunol. Methods* **2006**, *311* (1−2), 87−95.
(43) Chang, C. H.; Lai, Z. X.; Lin, H. L.; Yang, C. C.; Chen, H. H.; Yang, S. Y.; Horng, H. E.; Hong, C. Y.; Yang, H. C.; Lin, H. C. Use of Immunomagnetic Reduction for C-Reactive Protein Assay in Clinical Samples. *Int. J. Nanomed.* **2012**, *7*, 4335−4340.
(44) Yang, S. F.; Gao, B. Z.; Tsai, H. Y.; Fuh, C. B. Detection of C-Reactive Protein Based on a Magnetic Immunoassay by Using Functional Magnetic and Fluorescent Nanoparticles in Microplates. *Analyst* **2014**, *139* (21), 5576−5581.

https://doi.org/10.1021/acsomega.4c10064
ACS Omega 2025, 10, 10317−10326